SciPost Physics

Submission

A time-dependent momentum-resolved scattering approach to core-level spectroscopies

Krissia Zawadzki[1]
Alberto Nocera[2]
Adrian E. Feiguin[*3]

[1] School of Physics, Trinity College Dublin, College Green,
Dublin 2, Ireland
[2] Stewart Blusson Quantum Matter Institute, University of British Columbia,
Vancouver, British Columbia V6T 1Z4, Canada
[3] Department of Physics, Northeastern University,
Boston, Massachusetts 02115, USA
* a.feiguin@northeastern.edu

February 7, 2023

Abstract

While new light sources allow for unprecedented resolution in experiments with X-rays, a theoretical understanding of the scattering cross-section is lacking. In the particular case of strongly correlated electron systems, numerical techniques are quite limited, since conventional approaches rely on calculating a response function (Kramers-Heisenberg formula) that is obtained from a perturbative analysis of scattering processes in the frequency domain. This requires a knowledge of a full set of eigenstates in order to account for all intermediate processes away from equilibrium, limiting the applicability to small tractable systems. In this work, we present an alternative paradigm, recasting the problem in the time domain and explicitly solving the time-dependent Schrödinger equation without the limitations of perturbation theory: a faithful simulation of the scattering processes taking place in actual experiments, including photons and core electrons. We show how this approach can yield the full time and momentum resolved Resonant Inelastic X-Ray Scattering (RIXS) spectrum of strongly interacting many-body systems. We demonstrate the formalism with an application to Mott insulating Hubbard chains using the time-dependent density matrix renormalization group method, which does not require a priory knowledge of the eigenstates and can solve very large systems with dozens of orbitals. This approach can readily be applied to systems out of equilibrium without modification and generalized to other spectroscopies.

1 Introduction

Recent advances in experiments with light have paved the way to a new age in the study of elementary excitations of correlated matter [1–5]. High intensity X-ray sources, ultrafast pulses, and detectors with enhanced resolution for photon scattering measurements [1,4,6] have driven a continuous improvement of techniques such as X-ray absorption (XAS) and emission (XES) spectroscopies [7–9], resonant inelastic X-ray scattering (RIXS) [1, 4, 6, 10] as well as their corresponding dynamical versions (e.g. non-equilibrium or NE-XAS and time-resolved tr-RIXS). In particular, the possibility to probe with energy and momentum resolution excitations arising from charge, spin and orbital degrees of freedom has made RIXS the favorite tool to study the spectrum of solids and complex materials, including transition-metal compounds [11–15], Mott and anti-ferromagnetic insulators and unconventional high T_c superconductors [16–21].

This fruitful period has also been marked by theoretical efforts to understand more in depth the scattering processes and the nature of the dynamical correlation functions probed by these experiments [1]. In this respect, uncovering various aspects underlying the excitation spectrum of a system is associated to the calculation of dynamical correlation functions, a task that, to date, remains challenging. The limitations of available techniques to compute spectral properties in strongly correlated systems away from equilibrium has curbed further theoretical progress [22]. For instance, the Bethe Ansatz [23] and Dynamical Mean-Field Theory (DMFT) [24] are restricted to relatively simple model Hamiltonians, whereas time-dependent Density Functional Theory (TD-DFT) [8] covers weakly coupled regimes. Exact digonalization (ED), which has been the most employed numerical tool to calculate of the spectrum of solids and complex materials [10–14,25–39], provides access to small clusters and limits the momentum resolution.

The main limiting factor in these calculations is that core hole spectroscopies such as RIXS involve intermediate processes that can only be accounted for with an explicit knowledge of all the eigenstates of the system, requiring a full diagonalization of the Hamiltonian. Recently, Nocera *et al.* introduced a novel framework [40] based on the dynamical density matrix renormalization group (dDMRG) [41–43] aiming at extending the range of RIXS (and XAS) computations to systems beyond the reach of exact diagonalization (ED). Even though cluster sizes much bigger than ED were reached, the algorithm proposed in Ref. [40] requires a number of DMRG simulations scaling linearly in the size
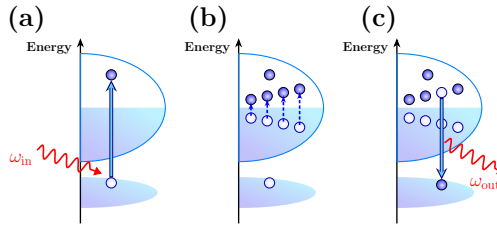
Figure 1: In a RIXS experiment, a core electron is excited into the valence band (a). After some time, an electron decays back into the core orbital, emitting a photon and leaving the system in an excited state, (b) and (c).

of the system, making the computation of the entire RIXS spectrum a difficult task for challenging Hamiltonians.

In this work, we propose an alternative approach in which the calculation of spectrum is recast as a scattering problem that can be readily solved by means the time-dependent DMRG method in a framework that does not require a full set of eigenstates of the Hamiltonian of the system. As we describe below, we explicitly introduce incident photons and core orbitals in the problem and numerically solve for the time evolution of the system accounting for the photon absorption and spontaneous emission in real time. This powerful formulation overcomes all the hurdles imposed by previous methods that work in the frequency domain and rely on explicitly obtaining dynamical spectral functions by means of generalized Fermi golden rules (Kramers-Heisenberg formula) in the frequency domain [44].

The paper is organized as follows: in Sec. 2 we review the principles of light-matter interactions taking place in X-ray experiments. With this foundation, we then introduce our approach and show how to recast the calculation of the spectrum as a time-dependent scattering problem. We describe a practical implementation for RIXS in Sec. 3. We present results using the time-dependent density matrix renormalization group method (tDMRG) [45–48] in Sec. 4 for a one-dimensional Mott insulator described by a Hubbard chain, a model which has been widely used to simulate RIXS in cuprates. Finally, we discuss our findings and implications in Sec. 5.

2 Light-matter interactions

We hereby briefly review the basic ideas describing an X-ray scattering experiment and provide a theoretical background to put the problem in context. Since X-rays are a highly energetic beam of photons, we represent them through a vector potential:

$$\mathbf{A}(\mathbf{r}) = \sum_{\mathbf{k},\lambda} A_{\mathbf{k}} \mathbf{e}_{\mathbf{k}\lambda}(b_{\mathbf{k}\lambda}e^{i\mathbf{k}\mathbf{r}} + b^{\dagger}_{\mathbf{k}\lambda}e^{-i\mathbf{k}\mathbf{r}}), \tag{1}$$

where $A_{\mathbf{k}} = \sqrt{2\pi c^2/V_s\omega_{\mathbf{k}}}$ is the normalized amplitude in volume V_s, with $\omega_{\mathbf{k}} = c|\mathbf{k}|$. The polarization unit vectors $\mathbf{e}_{\mathbf{k}\lambda}$ (λ=1,2) point in directions perpendicular to the propagation of the photons with momentum $\mathbf{k}$, represented by the conventional bosonic creation and annihilation operators $b^{\dagger}$, b. The full Hamiltonian including the solid and the radiation field is written as

$$H = H_0 + H_{ph} + V, \tag{2}$$

where H_0 describes the electrons and nuclei in the solid, and $H_{ph} = \sum_{\mathbf{k},\lambda} \omega_{\mathbf{k}}(b_{\mathbf{k},\lambda}^\dagger b_{\mathbf{k},\lambda} + 1/2)$. The light-matter interaction is given by

$$V = \frac{e}{mc} \sum_i \mathbf{p}_i \cdot \mathbf{A}(\mathbf{r}_i) + \frac{e}{2mc} \sum_i \sigma_i \cdot \nabla \times \mathbf{A}(\mathbf{r}_i), \tag{3}$$

where the first term accounts for the interaction of the electric field with the momentum $\mathbf{p}$ of the electrons and the second term describes the magnetic field acting on the electron spin σ. In the following, we will ignore the magnetic interaction as well as higher order terms that are not included in this expression. Therefore, replacing the quantized vector operator (1) leads to:

$$V = \frac{e}{mc} \sum_i \sum_{\mathbf{k},\lambda} A_{\mathbf{k}}(b_{\mathbf{k},\lambda}^\dagger \mathbf{e}_{\mathbf{k},\lambda} \cdot \mathbf{p}_i e^{i\mathbf{k}\mathbf{R}_i} + \text{h.c.}) \tag{4}$$

$$= \sum_{\mathbf{k},\lambda}(b_{\mathbf{k},\lambda}^\dagger D_{\mathbf{k},\lambda} + \text{h.c.}) \tag{5}$$

where we have assumed the dipole limit in which $e^{i\mathbf{k}\cdot\mathbf{r}} \simeq e^{i\mathbf{k}\cdot\mathbf{R}_i}$ where $\mathbf{R}_i$ is the position of the ion to which electron i is bound, and we have introduced the dipole operator

$$D_{\mathbf{k},\lambda} = \sum_i \frac{e}{mc} A_{\mathbf{k}} \mathbf{e}_{\mathbf{k},\lambda} \cdot \mathbf{p}_i e^{i\mathbf{k}\cdot\mathbf{R}_i}. \tag{6}$$

We start our discussion of the scattering processes by first considering a case in which a photon with momentum $\mathbf{k}$, energy $\omega_{\mathbf{k}}$ and polarization $\mathbf{e}_{\mathbf{k},\lambda}$ is absorbed, leaving the system energetically excited. The possible final states will be determined by the allowed dipolar transitions. In particular, one finds:

$$\langle n'l'm'|\mathbf{p}_i|nlm\rangle \neq 0 \iff \Delta l = \pm 1 \text{ and } \Delta m = 0, \pm 1$$

where $\Delta l = l' - l$ and $\Delta m = m' - m$, and l represents the orbital angular momentum with projection m. In the process we are interested in, this operator will create a core-hole excitation. In particular, we focus on the Cu L-edge ($2p \rightarrow 3d$) transition in a typical X-ray scattering experiment on a transition metal oxide cuprate material [49]. In this case,

$$D_{\mathbf{k},\lambda} = \sum_{i,\sigma,\alpha}(e^{i\mathbf{k}\cdot\mathbf{R}_i}\Gamma_\alpha^\lambda d_{i,\sigma}^\dagger p_{i,\alpha,\sigma} + \text{h.c.}), \tag{7}$$

where $d^\dagger$ adds an electron to the valence band ($3d_{x^2-y^2}$) and p_α creates a hole in a $2p_\alpha$ orbital. The coefficients Γ_α^λ are determined by the matrix elements of the dipole operator, $\Gamma_\alpha^\lambda \propto \langle 2p_\alpha|\mathbf{e}_{\mathbf{k},\lambda} \cdot \mathbf{r}|3d_{x^2-y^2}\rangle = 1$, where we have expressed the dipole operator in terms of the position operator $\mathbf{r}$ [1]. It is typically assumed that the core hole is strongly localized and only one Cu $2p_\alpha$ orbital is involved in the process.

After the excitation is created, the conduction electrons will experience a local Coulomb potential $-U_c$ in the presence of the core hole and Hamiltonian (2) is modified accordingly:

$$H = H_0 + H_c + H_{ph} + V, \quad H_c = -U_c \sum_i n_{di}(1 - n_{pi}),$$

$$V = V_{in} + V_{out}, \quad V_{out} = V_{in}^\dagger \tag{8}$$

$$V_{in} = \sum_{\mathbf{k},\lambda} b_{\mathbf{k},\lambda} D_{\mathbf{k},\lambda} = \sum_{\mathbf{k},\lambda} b_{\mathbf{k},\lambda} \sum_i e^{i\mathbf{k}\cdot\mathbf{R}_i} D_{i,\lambda},$$

with $D_{i,\lambda} = \sum_{\alpha,\sigma} \Gamma_\alpha^\lambda d_{i,\sigma}^\dagger p_{i\alpha,\sigma}$ and $n_p = \sum_\sigma p_\sigma^\dagger p_\sigma$, and it is important to notice that the p orbital can only be double or single occupied, but never empty since that would imply a two photon process.
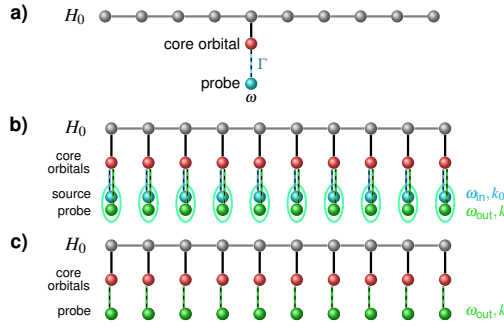
Figure 2: Schematic geometries used in the numerical calculations: (a) The local spectrum is measured adding one core orbital and emitted photon; (b) The momentum resolved RIXS calculation requires translational invariance, and an extended "detector" with one source and probe photon orbital per site; (c) in the semiclassical approach, the source photon is replaced by a classical field.

Due to the large local spin-orbit coupling in the core $2p$ orbital (of the order of 20eV at the Cu L-edge) the $2p$ orbitals split by their total angular momentum j, corresponding to the L_2 ($\tilde{j} = 1/2$) and L_3 ($\tilde{j} = 3/2$) transition edges. Because the energy separation between the two resonances is much larger than the core-hole lifetime broadening, we neglect the possibility of interference between the two edges, such that we have either $D_{\mathbf{k},\lambda} \simeq D_{\mathbf{k},\lambda,\tilde{j}=1/2}$ or $D_{\mathbf{k},\lambda} \simeq D_{\mathbf{k},\lambda,\tilde{j}=3/2}$. As a consequence, neither the spin nor the orbital angular momentum of the $2p$ band are good quantum numbers in the scattering process, but only the total angular momentum is conserved, allowing for orbital and spin "flip" processes at the Cu-L edge RIXS [10, 49]. We shall elaborate on this below.

3 Time-resolved RIXS

Resonant inelastic X-ray scattering (RIXS) is a high order process that can be described as a combination of X-ray absorption (XAS) and X-ray emission spectroscopy (XES), in which the system absorbs a photon with energy ω_{in} and emits another one with energy ω_{out}. We hereby focus on the so-called "direct RIXS" processes, see Fig.1 and Fig. 1 in Ref. [12]). As a consequence, the photon loses energy and the electrons in the solid end up in an excited state with momentum $\mathbf{k}' - \mathbf{k}$ and energy $\Delta\omega = \omega_{out} - \omega_{in}$. While in principle the resulting spectrum is a function of two frequencies, the incident photon ω_{in} is tuned to match one of the absorption edges, hence the resonant nature of the process. The final response is then determined by measuring the final occupation of the ω_{out} mode.

RIXS can be formulated in terms of a single photon being absorbed or emitted by the system. We consider the system locally connected to two photon orbitals, one with energy ω_{in} that will serve as the "source" for absorption, and a second one with energy ω_{out} will be the "detector" for emission and is initially empty. Since we are interested in obtaining the momentum resolved spectrum we need extended probe and sources [50]. This can be implemented in two different but equivalent setups, that we proceed to describe below.

3.1 Photon-in, photon-out description

In this setup, illustrated in Fig.2(b), each site will have a core-orbital, a source orbital, and a probe or detector orbital. Since the system is translational invariant, total momentum
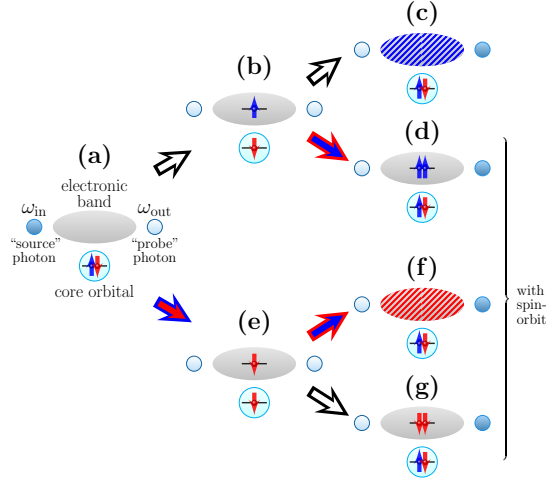
Figure 3: Depiction of the possible processes accounted for by our formulation of the direct RIXS problem: The incident photon has energy ω_{in}, and the "detector" is tuned to a target energy ω_{out}. The color arrows indicate processes in which a spin flip is involved, due to the spin orbit term. The (b)$\rightarrow$(c) path represents a process without spin orbit in which the final state of the band has the same quantum numbers as the original one. The (e) path corresponds to a spin-flip after absorption, while (d) and (f) undergo a spin-flip after emission. The final state can reverse the spin flip (d),(f) or leave the band with a different spin (c),(g). There is a similar cascade of processes related to these by time-reversal.

will be conserved. The problem is described by the Hamiltonian:

$$
\begin{aligned}
H &= H_0 + H_c + \omega_{in}\sum_i n_{b,s,i} + \omega_{out}\sum_i n_{b,d,i} + V, \\
V &= V_{in} + V_{out}; \;\; V_{out} = V_{in}^\dagger, \\
V_{in} &= \sum_{\sigma,\sigma'=\uparrow,\downarrow} V_{in}^{\sigma\sigma'} \\
V_{in}^{\sigma\sigma'} &= \sum_i (\Gamma_s^{\sigma\sigma'} b_{s,i} + \Gamma_d^{\sigma\sigma'} b_{d,i}) d_{i\sigma'}^\dagger p_{i\sigma}, \\
H_c &= -U_c \sum_{i\sigma}(1 - n_{pi\sigma}) n_{di},
\end{aligned}
\tag{9}
$$

where we have introduced couplings $\Gamma_{s/d}^{\sigma\sigma'}$ that can be turned on and off selectively depending of the case of interest, as we describe below. For instance, in the absence of spin-orbit interaction, only $\Gamma_{s/d}^{\sigma\sigma}$ will be non-zero. Otherwise, the spin projection is no longer a good quantum number and the core-electron is allowed to flip spin when it is excited.

At time $t = 0$, the problem is initialized with the core-orbitals double-occupied, the probe orbitals empty, and a single source photon with momentum $\mathbf{k}_{in}$. This can be done by means of a projector:

$$
H_{source} = -|\mathbf{k}_{in}\rangle\langle\mathbf{k}_{in}| + \lambda \sum_{ij} n_{b,s,i} n_{b,s,j},
$$

where the second term multiplied by a large positive constant $\lambda > 0$ represents a boson-boson repulsion that ensures that there is only one photon overall. This is necessary because the total Hamiltonian does not conserve photon number. We observe that since

there is only one photon at play, only one core-electron will be excited at most at any given time. The full calculation proceeds as follows: the energy ω_{in} is set to the transition edge and tDMRG simulations are carried out in parallel for each value of ω_{out}. The full spectrum is obtained by measuring the momentum distribution function of the detector at time t_{probe}, $n_{b,d}(\mathbf{k}) = 1/N^2 \sum_{mn} e^{i\mathbf{k}(\mathbf{R}_m - \mathbf{R}_n)} b_{d,m}^\dagger b_{d,n}$.

3.2 Semi-classical description

In order to reduce the computational complexity of the problem, we hereby introduce a semi-classical approach to completely eliminate the source degree of freedom. This alternative approach prescinds from the incoming photon and source orbitals and reduces the cost of the simulation exponentially.

The premise relies on the fact that –unlike spontaneous emission– the absorption process can be described semi-classically without using quantum photons by means of a classical field coupled to the dipole operator or, equivalently, in the form of a "gate potential":

$$
\begin{aligned}
H &= H_0 + H_c + \omega_{out} \sum_i n_{b,d,i} + \omega_{in} \sum_i n_{p,i} + V, \\
V &= V_{in} + V_{out}; \ V_{out} = V_{in}^\dagger, \\
V_{in} &= \sum_{\sigma,\sigma'=\uparrow,\downarrow} V_{in}^{\sigma\sigma'} \\
V_{in}^{\sigma\sigma'} &= \Gamma_d^{\sigma\sigma'} \sum_l b_{d,l}^\dagger d_{l\sigma'}^\dagger p_{l\sigma} + \Gamma_s^{\sigma\sigma'} \sum_l d_{l\sigma'}^\dagger p_{l\sigma}, \\
H_c &= -U_c \sum_{i\sigma} (1 - n_{pi\sigma}) n_{di},
\end{aligned}
\tag{10}
$$

where the "gate voltage" ω_{in} acts on all the core electronic states and we include a "hopping" term between the core states p and the conduction states d. Notice that this is a modification of the chain geometry, where the incoming photons are replaced by the voltage term. In our calculations we take ω_{in} corresponding to the XAS transition edge. As time evolves, due to energy and momentum conservation, core electrons with energy ω_{in} will be able to "tunnel" to the conduction/valence band, same as before. It can be easily shown that both formulations are mathematically equivalent, something that we have also corroborated numerically (not shown): results from the quantum and semi-classical approaches are indistinguishable.

An important consideration to take into account is that, since we are interested in a single photon process, only one core electron is can be excited to the conduction band at a time. This is naturally accounted for by the quantum mechanical formulation in Sec.3.1 with the source photons explicitly included. Therefore, the core orbitals can never be found empty, and only single and double occupied states are allowed. In practice, this can be done by either not including these states in the basis, or by adding a very large energy cost to states with empty core orbitals.

3.3 Measurement protocol

The goal is to measure the momentum distribution function of the detector $\langle \psi(t)|n_{b,d}(\mathbf{k})|\psi(t)\rangle$ after the scattering term is turned on (see Fig.2). We hereby focus on the implementation using the semi-classical description. Explicitly, one proceeds by carrying out a time-dependent simulation with the probe orbitals empty, and the core orbitals double occupied. The initial state of the electronic system may or may not be an eigenstate and
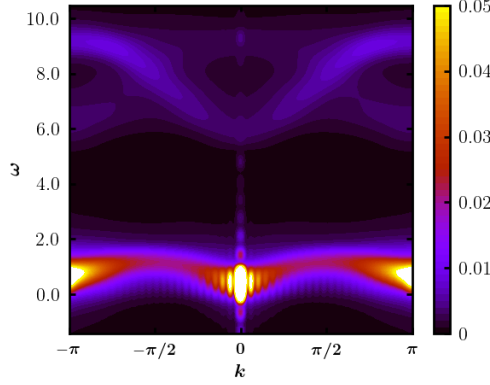
Figure 4: Momentum resolved RIXS spectrumn for a Hubbard chain with $U = 8$, $U_c = 1.5$, $\Gamma = 0.2$ and $L = 64$ sites, showing only the direct spin conserving channel using a Peierls phase replacing the source photon for the absorption process.

could be very far from equilibrium, since this approach applies regardless of the case. By setting $\Gamma_s^{\sigma\sigma'} = \Gamma_d^{\tau\tau'} = \Gamma$, and all others set to zero, one evolves the system in time to obtain a wave-function $|\psi_{\sigma\sigma',\tau\tau'}(t)\rangle$. The resulting contributions to the spectrum can be split into spin conserving and non-conserving ones:

$$I_{RIXS}^{\Delta S=0} = \langle \psi_{\uparrow\uparrow,\uparrow\uparrow} | n_{b,d} | \psi_{\uparrow\uparrow,\uparrow\uparrow} \rangle, \tag{11}$$

$$I_{RIXS}^{interference} = \langle \psi_{\uparrow\uparrow,\uparrow\uparrow} | n_{b,d} | \psi_{\downarrow\downarrow,\downarrow\downarrow} \rangle, \tag{12}$$

$$I_{RIXS}^{\Delta S=1} = \langle \psi_{\uparrow\uparrow,\downarrow\uparrow} | n_{b,d} | \psi_{\uparrow\uparrow,\downarrow\uparrow} \rangle. \tag{13}$$

The first expression, Eq.(11) involves the path (a)-(b)-(c) in Fig.3, while Eq.(12) the "interference" between this process and the one related by time-reversal symmetry with the "down" electron. The term Eq.(13) originates from the (a)-(b)-(d) channel, that results in a net spin flip in the conduction band in the presence of spin-orbit coupling. It is easy to see that these are the only distinct contributions, since all others are related by time-reversal symmetry.

By turning the couplings Γ on and off, this protocol allows us to measure each of the terms individually, including the interference Eq.(12) and the spin-flip contributions in Eq.(13). To account for all the terms, a total of four independent calculations would be required (notice that the interference term (12) involves two different wave-functions). However, setting all the $\Gamma_s^{\sigma\sigma'} = \Gamma_d^{\sigma\sigma'} = \Gamma$ will yield the total RIXS spectrum automatically from a single time-dependent simulation.

4 Results

4.1 Momentum resolved RIXS

With the probe extended to the entire volume of the system, we resolve the momentum dependence of the spectrum, as seen in Fig.4 (We show only results for the "direct" term, $I_{RIXS}^{\Delta S=0}$, Eq.(11)). We take $U = 8$, $U_0 = 1.5$ and tuned $\omega_{in} = 4.47$ to the transition edge for this value of U and kept 400 DMRG basis states. The dispersive features clearly allow us to identify different contributions. First, we note a bright low energy band that resembles the standard two-spinon continuum characterizing the low energy magnetic excitations
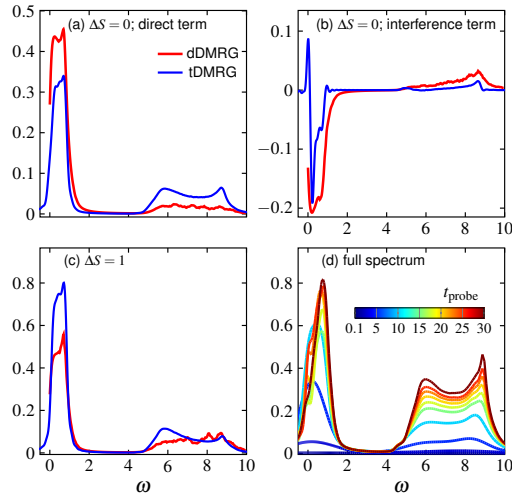
Figure 5: RIXS results using a time-dependent scattering approach for a Mott insulating Hubbard chain of length $L = 64$ with $U = 8$ and $U_c = 1.5$ and $t_{probe} = 30$. Panels show (a) the direct contribution, (b) interference term, (c) spin-flip term, and (d) full spectrum, also following its evolution as a function of time. dDMRG results are also shown for comparison.

spectrum of antiferromagnetic 1D spin-chain cuprates, such as Sr_2CuO_3 and $SrCuO_2$. These have been experimentally investigated both using RIXS at the Cu L-edge [49] and neutron scattering spectroscopy [51, 52]. Particularly evident is the sharp, large intensity peak at $k = 0$, $\omega = 0$ which represents the elastic peak, typical of RIXS experiments. We note that while this peak can easily be subtracted off in RIXS dDMRG calculations [53], this cannot be done in our tunneling approach, except in an ad-hoc way.

Finally, we highlight the upper excitation band at $\omega \in [6t, 10t]$, centered around $\omega \simeq 8t$, which describes particle hole (holon-doublon) excitations to the upper Hubbard band. Our results show a much better quality compared to dDMRG calculations at high energies, as in this case dDMRG precision deteriorates because it needs to converge over a big Krylov subspace [41, 54–56]. In particular, even though much less intense than the low energy spin excitation band, our approach can clearly resolve interesting features of the holon-doublon band, which can be fit by a cosine-like dispersion $E \simeq 8t - 2t\cos(k)$, plus an incoherent background at large momentum transfers. Our approach can therefore be of great help in the interpretation of RIXS experiments in low-dimensional cuprates where, besides magnetic excitations, also charge excitations play an important role, such as in correlated charge-density wave states [57, 58].

4.2 Single site spectrum

In order to gain more insight on the features and contributions at different energy scales, we now focus on a single site setup to calculate the local RIXS spectrum for the Mott insulating Hubbard chain. In this case, we use the geometry depicted in Fig.2(a), with a single core orbital and detector. Results obtained using the time-dependent scattering approach with $m = 300$ DMRG states are shown in Fig.5, compared to data obtained with dDMRG for the same system size and $m = 800$ states. The overall agreement is qualitatively very good, but the dDMRG results clearly suffer from poor precision particularly at high energies, as pointed out above. The discrepancies can be attributed to the fact that the time-evolved wave-function contains higher order contributions.

In agreement with the momentum resolved features described earlier, the resulting
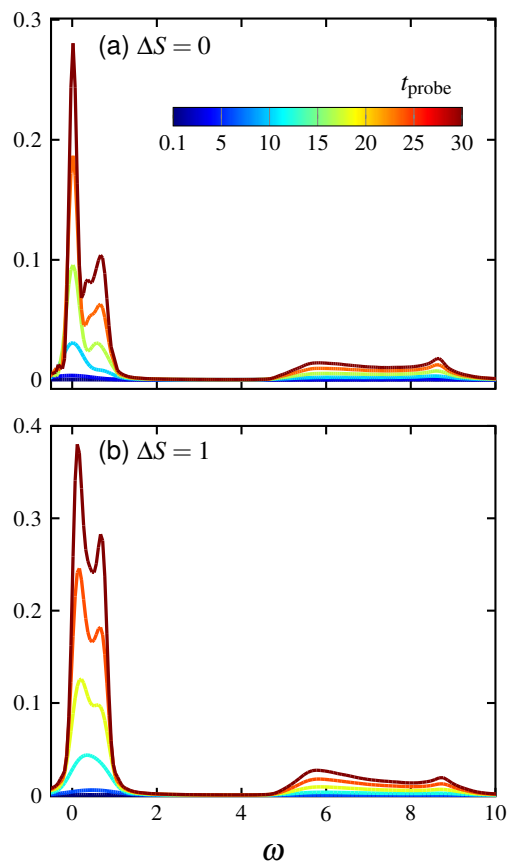
Figure 6: (a) Spin conserving and (b) non-conserving RIXS channels for a Mott insulating Hubbard chain with $U = 8$, $U_c = 1.5$, $\Gamma = 0.1$, $L = 64$ sites, for different probing times t_{probe}. The inelastic features at low energies emerge after a characteristic time for the electrons to break and decay into spinons and doublons.
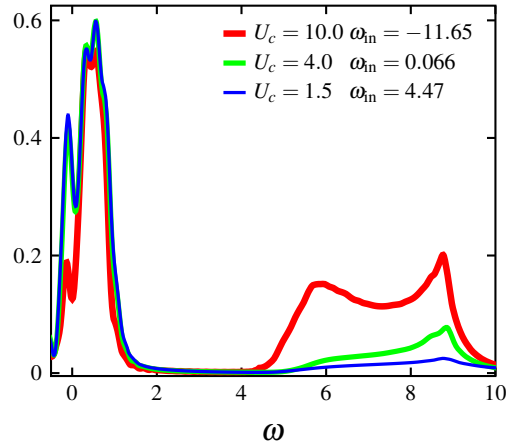
Figure 7: RIXS results (without spin-orbit interaction) for a Mott insulating Hubbard chain with $U = 8$, $L = 64$ sites, and different values of the core-hole potential U_c measured at time $t_{probe} = 30$.

spectrum contains signatures of a broad high-energy band, and a narrower low energy band with larger concentrated weight. The elastic contribution has been removed from the dDMRG data, implying that this low energy band indeed corresponds to spectral weight *in the gap*. While this can be confusing, it is readily explained in terms of multi spinon excitations with $\Delta S_z = 0$ produced by even number of spin flips and not changing the number of electrons [23]. While a Mott insulator has a charge gap, the spin excitations are gapless, a manifestation of spin-charge separation in one spatial dimension. Clearly, there are no available states within the Mott gap. The high energy features correspond to holon-doublon excitations that transfer spectral weight from the lower into the upper Hubbard band. In a Mott insulator away from equilibrium one can imagine high-order processes in which an electron in the band decays into the core orbital, simultaneously creating a particle hole excitation with an additional doublon in the upper Hubbard band. The decay of the doublon into spinons is unlikely, due to the weak spinon dispersion and the vanishing coupling between charge and spin [59–61](long doublon lifetime has also been observed in higher dimensions [62–65]).

4.3 Core-hole lifetime and dependence of the lineshape

The core-hole lifetime is in general also controlled by non-radiative decay mechanisms due to electronic correlations, such as Auger decay. Even though it is believed that the core-hole lifetime is an intrinsic property of atom, it was recently demonstrated that it can be tuned in certain cases by employing thin films x-ray planar cavities [66].

Unlike dDMRG, where the core-hole lifetime is introduced as an artificial damping in the Kramers-Heisenberg formula, in our approach the core-hole lifetime is an intrinsic property of the problem and is determined by the magnitude of the light-matter interaction Γ. In particular, the inverse core-hole *bare* linewidth for radiative decay is given by $\hbar\tau_{\text{core-hole}} = \pi \sum_{\mathbf{k}} |\Gamma_{\mathbf{k}}|^2 \delta(\epsilon_{\mathbf{k}} - \epsilon_c - \omega_{in})$, where $\epsilon_{\mathbf{k}}$ is the energy of the valence band electrons while ϵ_c is the core-level energy. [2]. In fact, the lifetime of the core-hole, while short, is actually momentum and energy dependent, and is intrinsically accounted for by our formulation. In our calculations, the lineshape for a fixed Γ will be determined by the time lapsing between the moment the photon source is turned on, and the emitted photon is measured by the detector, our t_{probe} for a smaller value of Γ. In Fig.6 we show RIXS results as a function of the probing time t_{probe}. As seen in Fig.6, different features evolve

with different characteristic times. At short times we observe the development of an elastic peak with little spectrum in the gap. This corresponds to an excitation being created at the transition edge and immediately recombining by emitting a photon, without energy loss and time to break into spinons, yielding only an elastic signal at $\omega = 0$. On the other hand, if we allow the system to evolve under the action of the core-hole potential between absorption and emission, the resulting attractive force will bind the doublon to the core orbital and create spin domain walls (spinons), that will propagate throughout the system. This is observed in the same figure, where the higher energy features in the spectrum evolve and become better resolved as we increase t_{probe}.

We point out that other factor that are not accounted by our formulation can play a role in the core-hole lifetime of actual materials, that can be very short due to non-radiative recombination mechanisms such as Auger [67, 68]. In our formulation, this effects could be included through a "core bath", as suggested in Ref. [69].

4.4   Dependence on the core-hole potential

Finally, we observe that the magnitude of U_c affects the relative spectral weight between the high and low energy bands. This is demonstrated in Fig.7, where we show the RIXS spectra obtained by varying U_c from 1.5 to 10. For large U_c, the core hole and a single doublon form a tightly bound state localized at the position of the core-orbital, effectively cutting the system in two. In the limit of $U_c \to \infty$, scattering with this potential induces holon-doublon excitations transferring weight into the upper Hubbard band, with a consequent increase in the spectral signal at high energies, while barely affecting the spectrum at low energies that originates from the spin degree of freedom.

Our numerical results can be understood in direct analogy with those obtained in indirect RIXS [70]: given the very small recombination rate of the holon-doublon after the absorption process, our data strongly suggest that the core-hole-holon-doublon bound state has a lifetime larger than the *bare* core-hole one. In fact, the doublon state is playing the role of the *spectator* (unoccupied) conduction band level in standard indirect RIXS. Indeed, in indirect RIXS, by increasing the core-level interaction U_c, and therefore increasing the incident energy at resonance, the spectral weight of charge (holon-doublon) excitations increases relative to that one of spin excitations.

5   Conclusions

We have introduced a time-dependent scattering approach to core-hole spectroscopies that allows one to carry out numerical calculations without the full knowledge of the excitation spectrum of the system. The applicability of the method is demonstrated by means of time-dependent DMRG calculations. Results for the Hubbard model are achieved with minimal effort on large systems using a fraction of the states –and simulation time– required by the dDMRG formulation. Unlike dDMRG and other approaches such as ED and DMFT that rely on explicitly calculating dynamical response functions based on the Kramers-Heisenberg formula, our time-dependent calculations are not limited by perturbation theory and contain contributions from higher order processes. Momentum resolution is obtained by means of extended source and probe, and an exponential speed up can be obtained by modeling the absorption process semi-classically by means of an oscillating field or, equivalently, of a "gate potential" term. In addition, our time-dependent approach can be readily applied without modification to non-equilibrium situations in which the electronic band is not in the ground state.

Our method differs from others in one notorious aspect: while the general approach essentially consists of first calculating a spectrum corresponding to an infinite core-hole lifetime, and then convoluting this spectrum with a Lorentzian lifetime broadening, in our time-dependent simulations there is no way to control the internal dynamics of the system and the core-hole lifetime is basically determined by the probing time t_{probe}. At long times we always observe the emergence of low energy states that can be associated to gapless multi-spinon excitations.

Our formulation opens the door to the numerical study of core-hole spectroscopies in strongly correlated systems away from equilibrium using exact many-body approaches such as as tDMRG. The results obtained by these means give one access to transient regimes and allow one to resolve different excitation and decay mechanisms in real time. These ideas can easily be implemented within other numerical frameworks, such as time-dependent DMFT.

6 Acknowledgments

We thank Shaul Mukamel for valuable feedback and Robert Markiewicz for stimulating discussions. We acknowledge generous computational resources provided by Northeastern University's Discovery Cluster at the Massachusetts Green High Performance Computing Center (MGHPCC). AN acknowledges the support from Compute Canada and the Advanced Research Computing at the University of British Columbia, where part of simulations were performed. AN is supported by the Canada First Research Excellence Fund. KZ was supported by a Faculty of the Future fellowship of the Schlumberger Foundation. AEF acknowledges the U.S. Department of Energy, Office of Basic Energy Sciences for support under grant No. DE-SC0014407.

References

[1] L. J. P. Ament, M. van Veenendaal, T. P. Devereaux, J. P. Hill and J. van den Brink, *Resonant inelastic x-ray scattering studies of elementary excitations*, Rev. Mod. Phys. **83**, 705 (2011), doi:10.1103/RevModPhys.83.705.

[2] F. de Groot and A. Kotani, *Core Level Spectroscopy of Solids*, Advances in Condensed Matter Science. CRC Press, ISBN 9781420008425 (2008).

[3] T. P. Devereaux and R. Hackl, *Inelastic light scattering from correlated electrons*, Rev. Mod. Phys. **79**, 175 (2007), doi:10.1103/RevModPhys.79.175.

[4] A. Kotani and S. Shin, *Resonant inelastic x-ray scattering spectra for electrons in solids*, Rev. Mod. Phys. **73**, 203 (2001), doi:10.1103/RevModPhys.73.203.

[5] Y. Wang, M. Claassen, C. D. Pemmaraju, C. Jia, B. Moritz and T. P. Devereaux, *Theoretical understanding of photon spectroscopies in correlated materials in and out of equilibrium*, Nature Reviews Materials **3**, 312 (2018), doi:10.1038/s41578-018-0046-3.

[6] J.-P. Rueff and A. Shukla, *A rixs cookbook: Five recipes for successful rixs applications*, Journal of Electron Spectroscopy and Related Phenomena **188**, 10 (2013), doi:https://doi.org/10.1016/j.elspec.2013.04.014, Progress in Resonant Inelastic X-Ray Scattering.

[7] F. De Groot, *High-resolution x-ray emission and x-ray absorption spectroscopy*, Chemical Reviews **101**(6), 1779 (2001).

[8] J. Rehr, *Theory and calculations of x-ray spectra: Xas, xes, xrs, and nrixs*, Radiation Physics and Chemistry **75**(11), 1547 (2006), doi:https://doi.org/10.1016/j.radphyschem.2005.11.014, Proceedings of the 20th International Conference on X-ray and Inner-Shell Processes.

[9] Y. Chen, Y. Wang, C. Jia, B. Moritz, A. M. Shvaika, J. K. Freericks and T. P. Devereaux, *Theory for time-resolved resonant inelastic x-ray scattering*, Phys. Rev. B **99**, 104306 (2019), doi:10.1103/PhysRevB.99.104306.

[10] C. Jia, K. Wohlfeld, Y. Wang, B. Moritz and T. P. Devereaux, *Using rixs to uncover elementary charge and spin excitations*, Phys. Rev. X **6**, 021020 (2016), doi:10.1103/PhysRevX.6.021020.

[11] K. Tsutsui, T. Tohyama and S. Maekawa, *Resonant inelastic x-ray scattering in one-dimensional copper oxides*, Phys. Rev. B **61**, 7180 (2000), doi:10.1103/PhysRevB.61.7180.

[12] S. Kourtis, J. van den Brink and M. Daghofer, *Exact diagonalization results for resonant inelastic x-ray scattering spectra of one-dimensional mott insulators*, Phys. Rev. B **85**, 064423 (2012), doi:10.1103/PhysRevB.85.064423.

[13] U. Kumar, A. Nocera, E. Dagotto and S. Johnston, *Multi-spinon and antiholon excitations probed by resonant inelastic x-ray scattering on doped one-dimensional antiferromagnets*, New Journal of Physics **20**(7), 073019 (2018), doi:10.1088/1367-2630/aad00a.

[14] U. Kumar, A. Nocera, E. Dagotto and S. Johnston, *Theoretical study of the spin and charge dynamics of two-leg ladders as probed by resonant inelastic x-ray scattering*, Phys. Rev. B **99**, 205130 (2019), doi:10.1103/PhysRevB.99.205130.

[15] Y. Wang, Y. Chen, C. Jia, B. Moritz and T. P. Devereaux, *Time-resolved resonant inelastic x-ray scattering in a pumped mott insulator*, arXiv preprint arXiv:1905.05405 (2019).

[16] L. Braicovich, J. van den Brink, V. Bisogni, M. M. Sala, L. J. P. Ament, N. B. Brookes, G. M. De Luca, M. Salluzzo, T. Schmitt, V. N. Strocov and G. Ghiringhelli, *Magnetic excitations and phase separation in the underdoped* $la_{2-x}sr_xcuo_4$ *superconductor measured by resonant inelastic x-ray scattering*, Phys. Rev. Lett. **104**, 077002 (2010), doi:10.1103/PhysRevLett.104.077002.

[17] M. Le Tacon, G. Ghiringhelli, J. Chaloupka, M. M. Sala, V. Hinkov, M. Haverkort, M. Minola, M. Bakr, K. Zhou, S. Blanco-Canosa *et al.*, *Intense paramagnon excitations in a large family of high-temperature superconductors*, Nature Physics **7**(9), 725 (2011).

[18] M. P. M. Dean, Y. Cao, X. Liu, S. Wall, D. Zhu, R. Mankowsky, V. Thampy, X. M. Chen, J. G. Vale, D. Casa, J. Kim, A. H. Said *et al.*, *Ultrafast energy- and momentum-resolved dynamics of magnetic correlations in the photo-doped mott insulator sr2iro4*, Nature Materials **15**(6) (2016), doi:10.1038/NMAT4641.

[19] D. G. Mazzone, D. Meyers, Y. Cao, J. G. Vale, C. D. Dashwood, Y. Shi, A. J. A. James, N. J. Robinson, J. Q. Lin, V. Thampy, Y. Tanaka, A. S. Johnson *et al.*, *Trapped transient magnons in the gapped antiferromagnet sr3ir2o7* (2020), 2002.07301.

[20] M. Dean, *Insights into the high temperature superconducting cuprates from resonant inelastic x-ray scattering*, Journal of Magnetism and Magnetic Materials **376**, 3 (2015), doi:https://doi.org/10.1016/j.jmmm.2014.03.057, Pseudogap, Superconductivity and Magnetism.

[21] H. Suzuki, M. Minola, Y. Lu, Y. Peng, R. Fumagalli, E. Lefrançois, T. Loew, J. Porras, K. Kummer, D. Betto *et al.*, *Probing the energy gap of high-temperature cuprate superconductors by resonant inelastic x-ray scattering*, npj Quantum Materials **3**(1), 65 (2018).

[22] R. S. Markiewicz, T. Das and A. Bansil, *Failure of $t-j$ models in describing doping evolution of spectral weight in x-ray scattering, optical, and photoemission spectra of cuprates*, Phys. Rev. B **82**, 224501 (2010), doi:10.1103/PhysRevB.82.224501.

[23] A. Klauser, J. Mossel, J.-S. Caux and J. van den Brink, *Spin-exchange dynamical structure factor of the $s = 1/2$ heisenberg chain*, Phys. Rev. Lett. **106**, 157205 (2011), doi:10.1103/PhysRevLett.106.157205.

[24] M. W. Haverkort, G. Sangiovanni, P. Hansmann, A. Toschi, Y. Lu and S. Macke, *Bands, resonances, edge singularities and excitons in core level spectroscopy investigated within the dynamical mean-field theory*, EPL (Europhysics Letters) **108**(5), 57004 (2014), doi:10.1209/0295-5075/108/57004.

[25] W. S. Lee, S. Johnston, B. Moritz, J. Lee, M. Yi, K. J. Zhou, T. Schmitt, L. Patthey, V. Strocov, K. Kudo, Y. Koike, J. van den Brink *et al.*, *Role of lattice coupling in establishing electronic and magnetic properties in quasi-one-dimensional cuprates*, Phys. Rev. Lett. **110**, 265502 (2013), doi:10.1103/PhysRevLett.110.265502.

[26] K. Okada and A. Kotani, *Zhang-rice singlet-state formation by oxygen $1s$ resonant x-ray emission in edge-sharing copper-oxide systems*, Phys. Rev. B **63**, 045103 (2001), doi:10.1103/PhysRevB.63.045103.

[27] C. Jia, E. Nowadnick, K. Wohlfeld, Y. Kung, C.-C. Chen, S. Johnston, T. Tohyama, B. Moritz and T. Devereaux, *Persistent spin excitations in doped antiferromagnets revealed by resonant inelastic light scattering*, Nat. Commun. **5** (2014).

[28] C. Monney, V. Bisogni, K.-J. Zhou, R. Kraus, V. N. Strocov, G. Behr, J. c. v. Málek, R. Kuzian, S.-L. Drechsler, S. Johnston, A. Revcolevschi, B. Büchner *et al.*, *Determining the short-range spin correlations in the spin-chain li_2cuo_2 and $cugeo_3$ compounds using resonant inelastic x-ray scattering*, Phys. Rev. Lett. **110**, 087403 (2013), doi:10.1103/PhysRevLett.110.087403.

[29] S. Johnston, C. Monney, V. Bisogni, K.-J. Zhou, R. Kraus, G. Behr, V. N. Strocov, J. Málek, S.-L. Drechsler, J. Geck, T. Schmitt and J. van den Brink, *Electron-lattice interactions strongly renormalize the charge-transfer energy in the spin-chain cuprate li_2cuo_2*, Nature Commun. **7**, 10563 (2016).

[30] F. Vernay, B. Moritz, I. S. Elfimov, J. Geck, D. Hawthorn, T. P. Devereaux and G. A. Sawatzky, *Cu k-edge resonant inelastic x-ray scattering in edge-sharing cuprates*, Phys. Rev. B **77**, 104519 (2008), doi:10.1103/PhysRevB.77.104519.

[31] C.-C. Chen, B. Moritz, F. Vernay, J. N. Hancock, S. Johnston, C. J. Jia, G. Chabot-Couture, M. Greven, I. Elfimov, G. A. Sawatzky and T. P. Devereaux, *Unraveling the nature of charge excitations in la_2cuo_4 with momentum-resolved cu k-edge resonant inelastic x-ray scattering*, Phys. Rev. Lett. **105**, 177401 (2010), doi:10.1103/PhysRevLett.105.177401.

[32] K. Okada and A. Kotani, *Copper k and oxygen k resonant inelastic x-ray scattering of one-dimensional cuprates*, J. Phys. Soc. Jpn. **75**, 044702 (2006).

[33] R. O. Kuzian, S. Nishimoto, S.-L. Drechsler, J. Málek, S. Johnston, J. van den Brink, M. Schmitt, H. Rosner, M. Matsuda, K. Oka, H. Yamaguchi and T. Ito, $Ca_2y_2cu_5o_{10}$: *The first frustrated quasi-1d ferromagnet close to criticality*, Phys. Rev. Lett. **109**, 117207 (2012).

[34] K. Tsutsui and T. Tohyama, *Incident-energy-dependent spectral weight of resonant inelastic x-ray scattering in doped cuprates*, Phys. Rev. B **94**, 085144 (2016), doi:10.1103/PhysRevB.94.085144.

[35] T. Tohyama, K. Tsutsui, M. Mori, S. Sota and S. Yunoki, *Enhanced charge excitations in electron-doped cuprates by resonant inelastic x-ray scattering*, Phys. Rev. B **92**, 014515 (2015), doi:10.1103/PhysRevB.92.014515.

[36] K. Ishii, K. Tsutsui, Y. Endoh, T. Tohyama, S. Maekawa, M. Hoesch, K. Kuzushita, M. Tsubota, T. Inami, J. Mizuki, Y. Murakami and K. Yamada, *Momentum dependence of charge excitations in the electron-doped superconductor* $nd_{1.85}ce_{0.15}cuo_4$: *A resonant inelastic x-ray scattering study*, Phys. Rev. Lett. **94**, 207003 (2005), doi:10.1103/PhysRevLett.94.207003.

[37] K. Tsutsui, T. Tohyama and S. Maekawa, *Mott gap excitations and resonant inelastic x-ray scattering in doped cuprates*, Phys. Rev. Lett. **91**, 117001 (2003), doi:10.1103/PhysRevLett.91.117001.

[38] M. A. van Veenendaal and G. A. Sawatzky, *Intersite interactions in cu l-edge xps, xas, and xes of doped and undoped cu compounds*, Phys. Rev. B **49**, 3473 (1994), doi:10.1103/PhysRevB.49.3473.

[39] C. Jia, C. Chen, A. Sorini, B. Moritz and T. Devereaux, *Uncovering selective excitations using the resonant profile of indirect inelastic x-ray scattering in correlated materials: observing two-magnon scattering and relation to the dynamical structure factor*, New Journal of Physics **14**(11), 113038 (2012).

[40] A. Nocera, U. Kumar, N. Kaushal, G. Alvarez, E. Dagotto and S. Johnston, *Computing Resonant Inelastic X-Ray Scattering Spectra Using The Density Matrix Renormalization Group Method*, Scientific Reports **8**, 11080 (2018), doi:10.1038/s41598-018-29218-8.

[41] A. Nocera and G. Alvarez, *Spectral functions with the density matrix renormalization group: Krylov-space approach for correction vectors*, Phys. Rev. E **94**, 053308 (2016), doi:10.1103/PhysRevE.94.053308.

[42] E. Jeckelmann, *Dynamical density-matrix renormalization-group method*, Phys. Rev. B **66**, 045114 (2002), doi:10.1103/PhysRevB.66.045114.

[43] T. D. Kühner and S. R. White, *Dynamical correlation functions using the density matrix renormalization group*, Phys. Rev. B **60**, 335 (1999), doi:10.1103/PhysRevB.60.335.

[44] K. Zawadzki, L. Yang and A. E. Feiguin, *Time-dependent approach to inelastic scattering spectroscopies in and away from equilibrium: Beyond perturbation theory*, Phys. Rev. B **102**, 235141 (2020), doi:10.1103/PhysRevB.102.235141.

[45] S. R. White and A. E. Feiguin, *Real-time evolution using the density matrix renormalization group*, Phys. Rev. Lett. **93**, 076401 (2004), doi:10.1103/PhysRevLett.93.076401.

[46] A. J. Daley, C. Kollath, U. Schollwöck and G. Vidal, *Time-dependent density-matrix renormalization-group using adaptive effective hilbert spaces*, Journal of Statistical Mechanics: Theory and Experiment **2004**(04), P04005 (2004), doi:10.1088/1742-5468/2004/04/p04005.

[47] A. E. Feiguin, *The density matrix renormalization group method and its time-dependent variants*, In *XV Training Course in the Physics of Strongly Correlated Systems*, vol. 1419, p. 5. AIP Proceedings (2011).

[48] S. Paeckel, T. Köhler, A. Swoboda, S. R. Manmana, U. Schollwöck and C. Hubig, *Time-evolution methods for matrix-product states*, Annals of Physics **411**, 167998 (2019), doi:https://doi.org/10.1016/j.aop.2019.167998.

[49] J. Schlappa, K. Wohlfeld, K. Zhou, M. Mourigal, M. Haverkort, V. Strocov, L. Hozoi, C. Monney, S. Nishimoto, S. Singh *et al.*, *Spin–orbital separation in the quasi-one-dimensional mott insulator sr 2 cuo 3*, Nature **485**(7396), 82 (2012).

[50] K. Zawadzki and A. E. Feiguin, *Time- and momentum-resolved tunneling spectroscopy of pump-driven nonthermal excitations in mott insulators*, Phys. Rev. B **100**, 195124 (2019), doi:10.1103/PhysRevB.100.195124.

[51] A. C. Walters, T. G. Perring, J.-S. Caux, A. T. Savici, G. D. Gu, C.-C. Lee, W. Ku and I. A. Zaliznyak, *Effect of covalent bonding on magnetism and the missing neutron intensity in copper oxide compounds*, Nature Physics **5**(12), 867 (2009).

[52] I. A. Zaliznyak, H. Woo, T. G. Perring, C. L. Broholm, C. D. Frost and H. Takagi, *Spinons in the strongly correlated copper oxide chains in* srcuo$_2$, Phys. Rev. Lett. **93**, 087202 (2004), doi:10.1103/PhysRevLett.93.087202.

[53] A. Nocera, F. H. L. Essler and A. E. Feiguin, *Finite-temperature dynamics of the mott insulating hubbard chain*, Phys. Rev. B **97**, 045146 (2018), doi:10.1103/PhysRevB.97.045146.

[54] A. Nocera, Y. Wang, N. D. Patel, G. Alvarez, T. A. Maier, E. Dagotto and S. Johnston, *Doping evolution of charge and spin excitations in two-leg hubbard ladders: Comparing dmrg and flex results*, Phys. Rev. B **97**, 195156 (2018), doi:10.1103/PhysRevB.97.195156.

[55] S. Li, A. Nocera, U. Kumar and S. Johnston, *Particle-hole asymmetry in the dynamical spin and charge responses of corner-shared 1d cuprates*, Communications Physics **4**(1), 1 (2021).

[56] A. Nocera and G. Alvarez, *Root-n krylov-space correction-vectors for spectral functions with the density matrix renormalization group*, arXiv preprint arXiv:2204.03165 (2022).

[57] P. Abbamonte, G. Blumberg, A. Rusydi, A. Gozar, P. Evans, T. Siegrist, L. Venema, H. Eisaki, E. Isaacs and G. Sawatzky, *Crystallization of charge holes in the spin ladder of sr14cu24o41*, Nature **431**(7012), 1078 (2004).

[58] L. Chaix, G. Ghiringhelli, Y. Peng, M. Hashimoto, B. Moritz, K. Kummer, N. B. Brookes, Y. He, S. Chen, S. Ishida *et al.*, *Dispersive charge density wave excitations in bi2sr2cacu2o8+ δ*, Nature Physics **13**(10), 952 (2017).

[59] K. A. Al-Hassanieh, F. A. Reboredo, A. E. Feiguin, I. González and E. Dagotto, *Excitons in the one-dimensional hubbard model: A real-time study*, Phys. Rev. Lett. **100**, 166403 (2008), doi:DOI: 10.1103/PhysRevLett.100.166403.

[60] L. G. G. V. Dias da Silva, K. A. Al-Hassanieh, A. E. Feiguin, F. A. Reboredo and E. Dagotto, *Real-time dynamics of particle-hole excitations in mott insulator-metal junctions*, Phys. Rev. B **81**, 125113 (2010), doi:10.1103/PhysRevB.81.125113.

[61] J. Rincón, K. A. Al-Hassanieh, A. E. Feiguin and E. Dagotto, *Photoexcitation of electronic instabilities in one-dimensional charge-transfer systems*, Phys. Rev. B **90**, 155112 (2014), doi:10.1103/PhysRevB.90.155112.

[62] R. Sensarma, D. Pekker, E. Altman, E. Demler, N. Strohmaier, D. Greif, R. Jördens, L. Tarruell, H. Moritz and T. Esslinger, *Lifetime of double occupancies in the fermi-hubbard model*, Phys. Rev. B **82**, 224302 (2010), doi:10.1103/PhysRevB.82.224302.

[63] M. Eckstein and P. Werner, *Thermalization of a pump-excited mott insulator*, Phys. Rev. B **84**, 035122 (2011), doi:10.1103/PhysRevB.84.035122.

[64] Z. Lenarčič and P. Prelovšek, *Ultrafast charge recombination in a photoexcited mott-hubbard insulator*, Phys. Rev. Lett. **111**, 016401 (2013), doi:10.1103/PhysRevLett.111.016401.

[65] M. Eckstein and P. Werner, *Ultra-fast photo-carrier relaxation in mott insulators with short-range spin correlations*, Scientific Reports **6**, 21235 EP (2016), Article L3 -.

[66] X.-C. Huang, X.-J. Kong, T.-J. Li, Z.-R. Ma, H.-C. Wang, G.-C. Liu, Z.-S. Wang, W.-B. Li and L.-F. Zhu, *Controlling core-hole lifetime through an x-ray planar cavity*, Phys. Rev. Research **3**, 033063 (2021), doi:10.1103/PhysRevResearch.3.033063.

[67] W. Bambynek, B. Crasemann, R. W. Fink, H. U. Freund, H. Mark, C. D. Swift, R. E. Price and P. V. Rao, *X-ray fluorescence yields, auger, and coster-kronig transition probabilities*, Rev. Mod. Phys. **44**, 716 (1972), doi:10.1103/RevModPhys.44.716.

[68] P. H. Citrin, G. K. Wertheim and Y. Baer, *Many-body processes in x-ray photoemission line shapes from li, na, mg, and al metals*, Phys. Rev. B **16**, 4256 (1977), doi:10.1103/PhysRevB.16.4256.

[69] M. Eckstein and P. Werner, *Simulation of time-dependent resonant inelastic x-ray scattering using nonequilibrium dynamical mean-field theory*, Phys. Rev. B **103**, 115136 (2021), doi:10.1103/PhysRevB.103.115136.

[70] J. van den Brink and M. van Veenendaal, *Theory of indirect resonant inelastic x-ray scattering*, Journal of Physics and Chemistry of Solids **66**(12), 2145 (2005), doi:https://doi.org/10.1016/j.jpcs.2005.10.168, 5th International Conference on Inelastic X-ray Scattering (IXS 2004).